IEEE Photonics Journal
An IEEE Photonics Society Publication

Open Access

# Loss-Tolerant Allpass-Based Filter Bank Design Suitable for Integrated Optics

Volume 6, Number 5, October 2014

**Yujia Wang, Student Member, IEEE**
**Ryan Aguinaldo, Member, IEEE**
**Truong Nguyen, Fellow, IEEE**

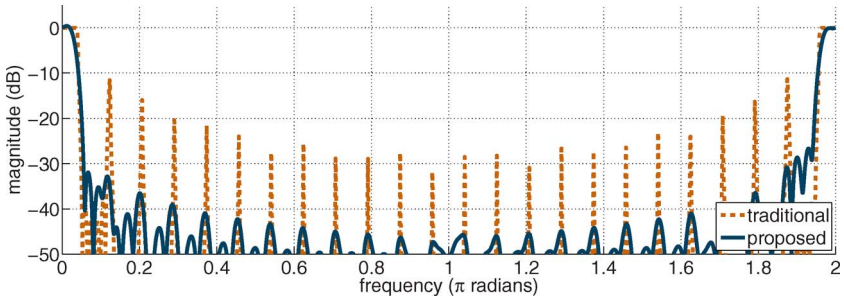


DOI: 10.1109/JPHOT.2014.2360301
1943-0655 © 2014 IEEE

IEEE photonics SOCIETY

IEEE

# Loss-Tolerant Allpass-Based Filter Bank Design Suitable for Integrated Optics

**Yujia Wang, *Student Member, IEEE*, Ryan Aguinaldo, *Member, IEEE*, and Truong Nguyen, *Fellow, IEEE***

Department of Electrical and Computer Engineering, University of California, San Diego, La Jolla, CA 92182 USA

*DOI: 10.1109/JPHOT.2014.2360301*


Manuscript received June 26, 2014; revised September 18, 2014; accepted September 20, 2014. Date of publication September 25, 2014; date of current version October 1, 2014. This work was supported in part by the National Science Foundation under Grant CCF-1065305. Corresponding author: Y. Wang (e-mail: yuw041@ucsd.edu).

**Abstract:** This paper presents a novel design algorithm for a filter bank structure that is suitable for photonic integrated circuits. The proposed design is entirely based on the principle of loss-exhibiting allpass filtering, which is a behavior naturally observed in a variety of microscale optical components. The setup and mathematical optimization of the system is explored in detail from a signal processing perspective, and an algorithm based on convex and nonlinear optimization techniques is subsequently presented. The algorithm methodologically utilizes the otherwise-undesirable effect of waveguide loss to derive an allpass-based filter bank structure that is amenable to photonic implementation. The proposed structure is ideal for applications in time-stretched analog-to-digital converters, WDM network channelizers, and general optical signal multiplexers.

**Index Terms:** Filter bank, allpass filter, waveguide loss, ring resonator, filter design.

## 1. Introduction

Integrated optical platforms, such as silicon photonics, have been used in a wide variety of filtering [1], multiplexing [2], and switching [3] schemes. As system complexity of these optical circuits increases, algorithmic design methods become a necessity. In particular, the concurrent derivation of multiple filter responses, in terms of an optimal filter bank, is critical in enabling sub-band processed photonic circuits for advanced applications such as time-stretched ADCs [4] and multiplexing in high density WDMs [5]. In contrast to previous filter design methods, as discussed below, we invoke a design algorithm based on the theory of filter banks and allpass processing. Furthermore, since the fabrication of true allpass filters is practically unrealizable in silicon photonics [6], we continue in the spirit of our previous work [7], [8] by showing that the allpass-based design method can handle the realistic impairment of unavoidable waveguide loss in the photonic "allpass" filter.

A significant amount of effort has been put into the design of photonic bandpass filters that exhibit desirable passband and stopband behaviors [9]–[11]. While it is possible to extend these designs to filter banks by frequency tuning, it is well known from a signal processing perspective that such approach is sub-optimal due to concerns regarding performance optimality, implementation complexity, and uniformity [12]. With such premise, the systematic design of

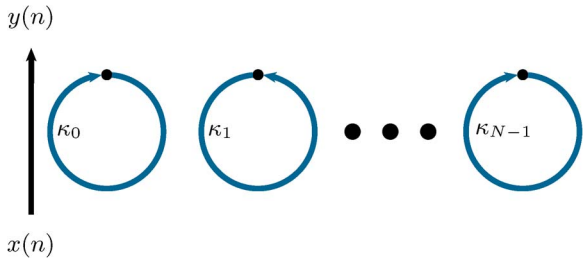


Fig. 1. *N*th order lattice allpass filter based on rings. Each pair of adjacent rings produces induced coupling, which serves as a four-port interface.

photonic filter banks started to show development [13]–[15]. The design of filter banks has long been a major research topic in digital signal processing, and a variety of different structures are available to best suit the needs of a wide range of communication applications. Existing photonic based designs, however, can often be categorized as multi-level filter bank structures that are susceptible to progressively degrading performances as the number of channels increase. The benefit to a filter bank that can guarantee uniformity across channels is therefore immediately evident.

The allpass-based DFT filter bank [16] is a particularly interesting structure for photonic realization due to its connection to the CROW [17] and FBG [18] architectures. In addition to their robustness to errors and low power consumption, allpass based structures are known to provide the lowest implementation and computation complexity [19]. Such characteristics directly translate to relaxed fabrication requirements in photonic implementation. While it is tempting to directly leverage off the existing design concept, the original architecture is structurally dependent on additional processing to be functional in the electrical and digital domain. At the same time, design methods that should carry over from DSP are plagued by the provision of non-ideal filter elements from the optical platform.

Loss characterization of both passive [6], [20] and active [3] silicon photonic components have become commonplace since such loss is fundamentally unavoidable due to fabrication limitations that induce scattering [21], additional scattering at waveguide bends and transitions [6], and free carrier absorption [22]. In this paper, we present a design method that intelligently utilizes the characterization of waveguide power loss to eliminate the need for additional filtering in the original structure. The presented method subsequently demonstrates the optimality of allpass-based filter bank exclusive to photonic implantation.

The rest of the paper is outlined as follows: Section 2 provides a signal processing analysis of the allpass filter and demonstrates its connection to nanoscale photonic elements. The effect of waveguide loss is also carefully explained in this section. Section 3 details the theory and drawbacks of the traditional DFT allpass based filter bank. Section 4 proposes the modified structure and explains the approach to the algorithm development. Section 5 shows the simulation results, and Sections 6 concludes the paper.

## 2. Allpass Filters

An allpass filter is a system that exhibits no attenuation on the input signal's power, but alters the phase based on a designed behavior. The structure is widely used in signal processing and communication, and has been demonstrated to be excellent for optical applications such as group delay equalization and dispersion compensation. An optical allpass filter can be easily realized using a number of basic nanoscale photonic elements such as ring resonators [23]. Consider the ring based lattice architecture shown in Fig. 1. Under ideal fabrication, the power of the input signal $x(n)$ is entirely contained within the structure, despite the obvious processing from the traversal of the optical signal and coupling. Also notice that we can observe the same behavior for a cascade configuration.

### 2.1 Ideal Behavior

The structure shown in Fig. 1 can be directly linked to the canonical representation of a $N$th-order allpass filter from signal processing. The transfer function for an $N$th-order photonic allpass filter is [24]

$$A(z) = (-1)^N \frac{d_N^* + d_{N-1}^* z^{-1} + \cdots d_1^* z^{-(N-1)} + z^{-N}}{1 + d_1 z^{-1} + \cdots d_{N-1} z^{-(N-1)} + d_N z^{-N}} = (-1)^N z^{-N} \frac{D^*(1/z^*)}{D(z)} \tag{1}$$

where $d_i$'s are the filter coefficients and are related to the coupling coefficients $\kappa_i$'s through the lattice synthesis equation or polynomial factorization. Recall that $z = re^{j\omega}$, and the transfer function $A(z)$ describes a system's behavior under all complex numbers. The unit delay $z^{-1}$ is associated with the minimum amount of time between two observable instances of the signal in the system. Notice that the system exhibits no processing on the input signal's power because the magnitudes of $D(z)$ and $D^*(1/z^*)$ are the same. The phase response of $A(z)$, however, is controllable and is governed by

$$\Theta_{\hat{A}}(\omega) = -N\pi - N\omega - 2 \arctan \frac{\Im\{D(e^{j\omega})\}}{\Re\{D(e^{j\omega})\}}. \tag{2}$$

The phase response of an allpass filter is therefore dependent on the placements of the roots of $D(z)$. Note that for every root $p_i$ of $D(z)$, there exists a zero $z_i$ from $D^*(1/z^*)$ at $z_i = 1/p_i^*$. Since precise placements of the roots of $D(z)$ depend on the values of the filter coefficients of $D(z)$, $d_i$'s are the ultimate control variables that need to be optimized for a given prescribed requirement.

### 2.2 Effect of Waveguide Power Loss

In photonic implementation, the waveguide loss effect is inescapable under realistic considerations of the material and fabrication process. For example, a single ring resonator, coupled to a single bus waveguide, exhibits a rich spectrum of resonant nulls [20]. These resonances, however, occur because of the presence of loss in the ring. If the loss were absent, the ring resonator would impart a spectrally varying phase shift onto the light, but with unity transmission; i.e., an allpass filter would be realized. To properly consider the design of photonic filters, the integration of loss into the design is therefore necessary. The effect of loss can be captured by

$$\gamma = e^{-\alpha L/2} \tag{3}$$

where $\alpha$ is the power attenuation coefficient of the waveguide, and $L$ is the length of the ring. Note that while there is a degree of randomness to $\gamma$, we will assume the effect can be expressed by a nominal value that is known *a priori*, which is expected under stable fabrication conditions [25]. Since the power loss occurs as the optical signal traverses through the waveguide, it is coupled with the unit delay $z^{-1}$, the response of a photonic allpass filter under waveguide power loss is

$$\hat{A}(z) = A(\gamma^{-1} z). \tag{4}$$

The effect on the magnitude and phase responses of the allpass filter is shown in Fig. 2. The loss distorts the phase and causes the magnitude response to exhibit concavities at the frequencies of the roots. Note that it is also possible to consider the wavelength dependency of $\gamma$ simply by expressing the loss as a function $\gamma(\omega)$. While these effects are generally undesirable, they can be utilized to enable the realistic implementation of photonic allpass filter banks.

## 3. DFT Allpass Filter Bank

A bank of filters is an effective, and often necessary, approach to segmenting a wideband signal into multiple subbands for processing. In general, in a $M$-band filter bank, we seek to jointly design $M$ bandpass filters with equal bandwidth.

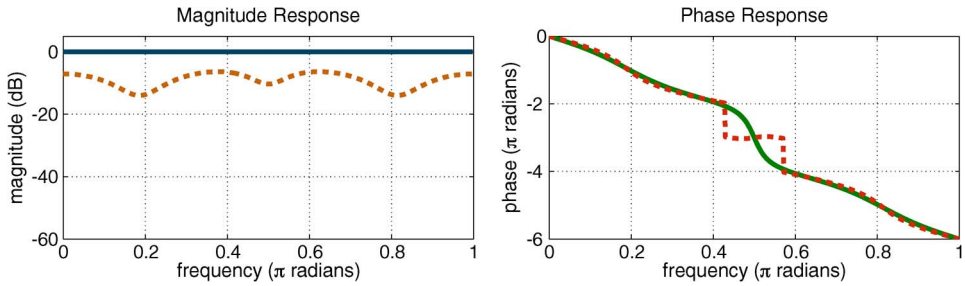


Fig. 2. Effect of $\gamma = 0.9$ on the magnitude (left) and phase (right) responses of a 6th-order allpass $\hat{A}(z)$. The solid lines are the ideal responses.

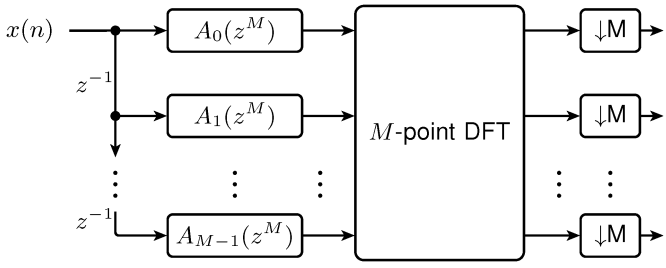


Fig. 3. Four-channel allpass based filter bank signal flow diagram. The downsample and filtering operations in this structure are interchangeable, allowing for efficient implementation and processing.

### 3.1 Structure

Here, we consider the allpass based filter bank [16] shown in Fig. 3. One key aspect in this structure is the ability to switch the filtering and downsample operations. In signal processing, such feature is extremely beneficial because it implies that a wideband signal can effectively be processed at sub-Nyquist sampling rates. In optical signals, the essence of downsampling can be observed in the process of time stretching. An optical signal slowed by a stretch factor of $M$ has its bandwidth reduced by a factor of M, which indicates that the signal can be sampled by $f_s/M$, where $f_s$ is the original Nyquist sampling rate. The operation directly maps to downsampling since the purpose of a downsample by $M$ operation is exactly to reduce the sampling rate to $f_s/M$.

While the structure does not explicitly process the input signal through independent bandpass filters, the outputs are exactly the sub-band signals of $x(n)$. The implicit analysis filters of this structure can be expressed as

$$H_i(z) = \frac{1}{M}\sum_{k=0}^{M-1} e^{-j2\pi\frac{i\cdot k}{M}} A_k(z^M) z^{-k}. \tag{5}$$

It is often desirable to ensure that $A_0(z^M)$ is a simple delay because such formulation would provide constant group delay in the passband regions for all bands. For example, the analysis filters for a 4-channel filter bank are

$$\begin{bmatrix} H_0(z) \\ H_1(z) \\ H_2(z) \\ H_3(z) \end{bmatrix} = \frac{1}{4}\begin{bmatrix} 1 & 1 & 1 & 1 \\ 1 & -j & -1 & j \\ 1 & -1 & 1 & -1 \\ 1 & j & -1 & -j \end{bmatrix}\begin{bmatrix} z^{-4N} \\ A_1(z^4)z^{-1} \\ A_2(z^4)z^{-2} \\ A_3(z^4)z^{-3} \end{bmatrix} \tag{6}$$

where $N$ is the order of the allpass filters after downsample.

Since the allpass filters have no controllable behavior in the magnitude, the system operates based on the principle of phase matching. Given the phase profile $\Theta_0(M\omega)$ of $A_0(z^M)$, a passband in $H_0(z)$ can be created by requiring the rest of the allpasses to have the same phase in

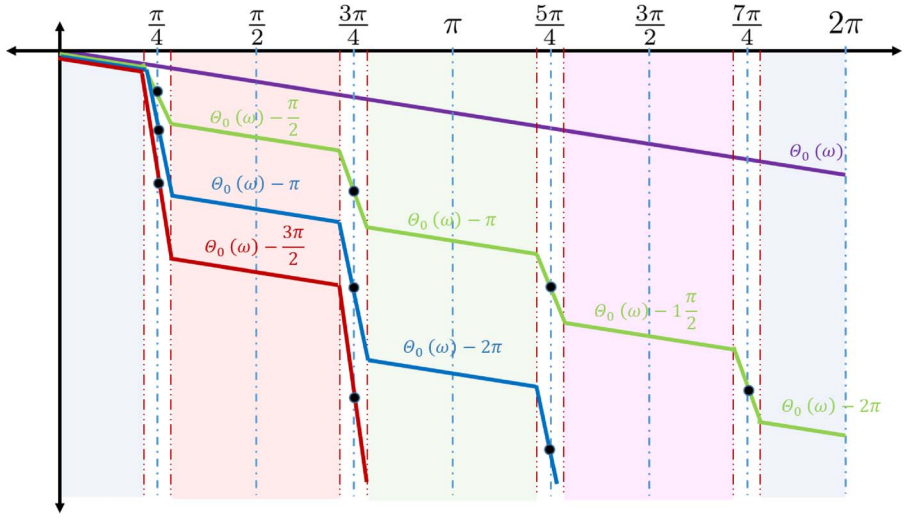


Fig. 4. Phase requirements for $A_k(z^M)z^{-k}$ in a $M = 4$-channel DFT filter bank. Note that $A_0(z^M)$ is assumed to be a delay.

$0 \leq \omega \leq \omega_p$, where $\omega_p$ is the passband frequency. A stopband can be created in a similar fashion by requiring a phase offset of $\pi$. An example phase requirement for a 4-channel filter bank is shown in Fig. 4. Notice that there is a required phase increment in each of the allpass filters at $(2k+1)\pi/4$. In general, the prescribed phase $\Theta_k(\omega)$ for each $A_k(z^M)z^{-k}$ pair in a $M$-channel filter bank is

$$\Theta_k(\omega) = -MN\omega - \frac{2\pi(l+1)k}{M}, \quad \omega_{p,l} \leq \omega \leq \omega_{s,l} \tag{7}$$

where $\omega_{p,l}$ and $\omega_{s,l}$ are the start and end points of the $l$th band. Given a prescribed requirement $\Theta_{pre}(\omega)$, the allpass filters can be designed using a variety of existing algorithms such as the eigenfilter method [26].

### 3.2 Limitations

An example prototype filter $H_0(z)$ from a 4-channel DFT allpass structure is shown in Fig. 5. Note that the other $H_i(z)$'s are simply frequency shifted versions of $H_0(z)$ with the exact same performances. Notice that the resulting $H_0(z)$ exhibits an undesirable spur at $\omega_c = 3\pi/4$, and the effect also propagates to the rest of the channels due to symmetry. Such behavior is highly undesirable since it severely limits the overall Spurious-Free Dynamic Range (SFDR) of the overall system, and may cause cross-talk in communication structures.

The effect, however, is inherent to the structure and cannot be addressed through design. For each allpass pair $A_k(z^M)z^{-k}$, the structure requires a phase discontinuity of $2\pi(l+1)k/M$ between two adjacent frequency bands of interest $l$ and $l+1$. Such requirement would also imply that at the corner frequencies $\omega_{c,l} = (2l+1)\pi/M$, the phase response of the $k$th allpass is approximately

$$\Theta_k\left(\frac{2\pi(l+1)}{M}\right) \approx -MN\omega - \frac{1}{2}\cdot\frac{2\pi(l+1)k}{M}. \tag{8}$$

In other words, the frequency response $H_0(e^{j\omega})$ at the corner frequencies can be expressed as

$$H_0(e^{j\omega_{c,l}}) \approx \frac{1}{M}e^{j\Theta_0(M\omega_{c,l})}\sum_{k=0}^{M-1} e^{-j\frac{\pi(l+1)k}{M}}. \tag{9}$$

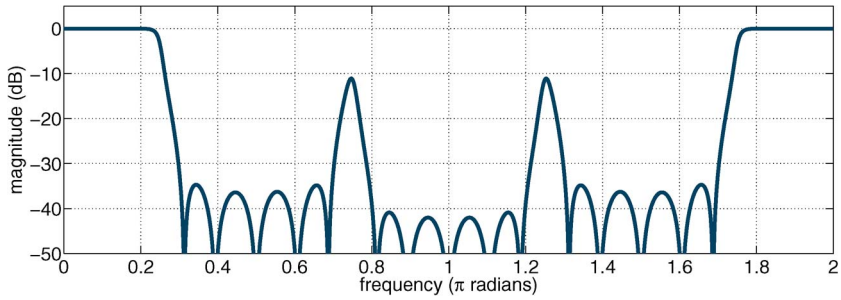


Fig. 5. Magnitude response of $H_0(z)$ in a 4-channel DFT allpass filter bank. The baseline allpass filter $A_0(z)$ is chosen as a simple delay $A_0(z^4) = z^{-4\cdot 2}$ and $\omega_p = 0.2\pi$.

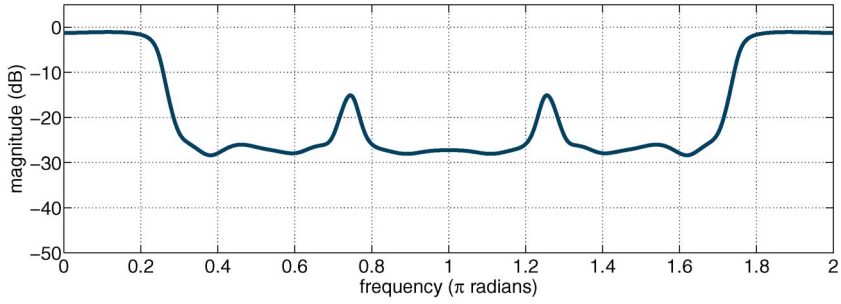


Fig. 6. Magnitude response of $H_0(z)$ in a 4-channel DFT allpass filter bank when implemented using photonic elements with a loss of $\gamma = 0.97$. Note that the delay element is assumed to have negligible loss.

Since the amount of the phase change is governed by the DFT structural setup, it is a rigid requirement and cannot be modified. In electrical implementations of the DFT allpass filter bank, this drawback is addressed by introducing an additional interpolation filter to cancel the spurs [16]. Such approach, however, would imply additional hardware and, therefore, may not always be feasible.

## 4. Proposed Design Algorithm

While the effect of the spurs cannot be avoided, photonic implementation may present itself as the optimal platform for the DFT allpass filter bank since optical setups naturally mitigates the effect. Recall that in photonic signal processors, the effect of waveguide power loss must always been considered. The magnitude response of the baseband filter $H_0(z)$ when implemented using photonic allpass filters with a loss of $\gamma = 0.97$ is shown in Fig. 6. While the power loss seems to simply result in a degradation of the response, its effect can be harnessed and used in place of any additional follow-up filter.

The benefit of the waveguide loss in a DFT filter bank can be understood from examining the poles and zeros of the allpass filters. The poles and zeros of the allpass filters in the 4-channel filter bank example are shown in Fig. 7. Notice that in each $A_k(z^M)$, there exists a pole zero pair in close proximity to the unit circle at $\omega = (2l + 1)\pi/M$. Such condition is guaranteed regardless of design specifications due to the specific requirements on the staircase behaviors of the phase responses. The existence of these roots at the corner frequencies can be utilized in conjunction with the loss effect to produce optimal filter bank design for photonic implementation.

The waveguide loss changes the frequency response of an allpass filter to $A_k(\gamma^{-1}z)$, which can be viewed as shifting the roots of the ideal allpass towards the origin. Such effect causes the allpass to lose the precise balance of having each pole zero pair at radii $r_n$ and $1/r_n$. As a zero approaches the unity circle in the $z$-plane, the magnitude response would then exhibit a

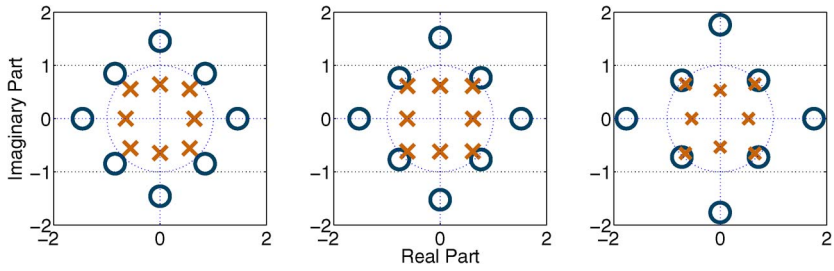


Fig. 7. Poles and zeros of the allpass filters $A_k(z^4)$ in a 4-channel filter bank prior to considering the effect of waveguide power loss.

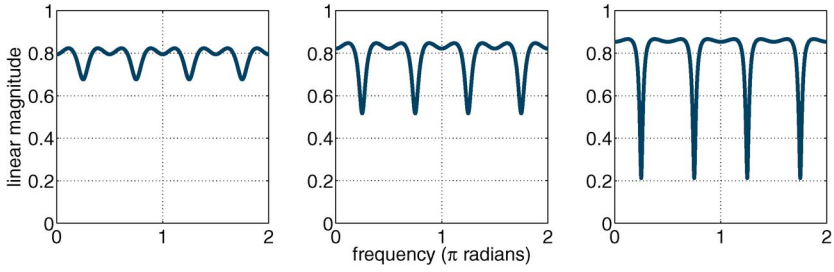


Fig. 8. Magnitude responses of the allpass filters under waveguide loss $\gamma = 0.97$ in a 4-channel filter bank.

concavity. The effect of $\gamma = 0.97$ on the allpass filters' magnitude responses in the 4-channel example is shown in Fig. 8. Notice that the loss causes each of the allpass filters $A_k(z^M)$'s to exhibit a strong null at $(2l+1)\pi/4$ due to the pole zero pair at close proximity to the unit circle. The locations of these nulls exactly align with the spurs in the analysis filters $H_i(z)$'s. A photonic implementation therefore naturally offers a means to mitigating the undesirable effects in a DFT allpass filter bank. However, the effect of $\gamma$ is not uniform for all of the allpass filters and must be properly optimized.

In the original structure setup, each of the allpass filters is given a weight of $1/M$ due to equal magnitude contributions. Under loss, the nominal levels of the allpass magnitude responses are no longer equal, as seen in Fig. 8. A first step in designing the photonic filter bank is therefore to redistribute the weights. The analysis filter responses for the proposed structure takes the form

$$H_i(z) = \sum_{k=0}^{M-1} W_k e^{-j2\pi\frac{i\cdot k}{M}} A_k(\gamma^{-M} z^M) z^{-k} \tag{10}$$

where $W_k$'s are weights that are optimized for a given loss parameter $\gamma$. Note that the redistribution does not cause additional insertion loss because the input signal's power is entirely contained within the system. Since the $M$ analysis filters are identical, it is sufficient to optimize $W_k$'s for $H_0(z)$. Using the designed allpass coefficients from the lossless setup, let us first formulate

$$\mathbf{a}(e^{j\omega}) = \begin{bmatrix} e^{-jNM\omega} \\ A_1(\gamma^{-M} e^{jM\omega}) e^{-j\omega} \\ \vdots \\ A_{M-2}(\gamma^{-M} e^{jM\omega}) e^{-j(M-2)\omega} \\ A_{M-1}(\gamma^{-M} e^{jM\omega}) e^{-j(M-1)\omega} \end{bmatrix} \tag{11}$$

where $A_k(\gamma^{-M} e^{jM\omega})$ is the allpass response under loss obtained using the coefficients derived from the ideal allpass filter bank setup.

The goal of the $W_k$'s is to counterbalance the uneven nominal magnitude responses of the allpass filters, we therefore formulate the following optimization setup

$$\begin{aligned} \underset{\mathbf{w}}{\text{minimize}} \quad & \left\|\mathbf{w}^T\mathbf{a}(e^{j\omega})\right\|_2^2 \\ \text{subject to} \quad & \mathbf{w}^T\mathbf{1} = 1 \\ & \mathbf{w} > 0 \end{aligned} \tag{12}$$

for $\omega_s \leq \omega \leq \pi$, where $\mathbf{w} = [W_0 \ W_1 \ \cdots \ W_{M-1}]^T$. The optimization setup is equivalent to maximizing the stopband attenuation for $H_0(z)$. Note that the passband is neglected because the general shape of the response is already determined by the allpass coefficients. The stopband profile, however, depended on magnitude cancellation through phase matching, and therefore must be readjusted. The formulation conforms to a least squares setup and can be easily solved.

By recalculating the weights, we are able to enhance the resolution between the passband and stopband of $H_0(z)$. However, the spurs still exist and limit the filter performance. To remove the spurs, we must optimize the filter coefficients specifically for photonic implementation. Under waveguide power loss $\gamma$, the frequency response of $H_0(z)$ is

$$H_0(\mathbf{e}^{j\omega}) = W_0\mathrm{e}^{-jNM\omega} + \sum_{k=1}^{M-1} W_k \frac{\mathbf{d}^T\mathbf{J}\mathbf{e}(\gamma^M\mathrm{e}^{jM\omega})}{\mathbf{d}_k^T\mathbf{e}(\gamma^M\mathrm{e}^{jM\omega})\mathrm{e}^{-jk\omega}}. \tag{13}$$

Let

$$\mathbf{d} = \begin{bmatrix} \mathbf{d}_1^T & \mathbf{d}_2^T & \cdots & \mathbf{d}_{M-2}^T & \mathbf{d}_{M-1}^T & \mathbf{w}^T \end{bmatrix}^T \tag{14}$$

$$\mathbf{I}_k = \begin{bmatrix} \mathbf{0}_{(k-1)N\times N} \\ \mathbf{I} \\ \mathbf{0}_{(M-2-k)N\times N} \\ \mathbf{0}_{M\times N} \end{bmatrix}, \quad \mathbf{M}_k = \begin{bmatrix} \mathbf{0}_{(M-1)\times N} \\ \mathbf{0}_{k\times N} \\ 1 \\ \mathbf{0}_{(M-1-k)\times N} \end{bmatrix}. \tag{15}$$

The frequency response $H_0(\mathrm{e}^{j\omega})$ can be expressed in vector matrix notations as

$$H_0(\mathbf{e}^{j\omega}) = \mathbf{d}^T\mathbf{M}_0\mathrm{e}^{-jNM\omega} + \sum_{k=1}^{M-1} \mathbf{d}^T\mathbf{M}_k \frac{\mathbf{d}^T\mathbf{I}_k\mathbf{J}\mathbf{e}(\gamma^M\mathrm{e}^{jM\omega})}{\mathbf{d}_k^T\mathbf{I}_k\mathbf{e}(\gamma^M\mathrm{e}^{jM\omega})\mathrm{e}^{-jk\omega}}. \tag{16}$$

The overall design goal is

$$\underset{\mathbf{d}}{\text{minimize}} \quad \left\| \left|H_0(\mathrm{e}^{j\omega})\right|^2 - D(\omega) \right\|_\infty \tag{17}$$

where

$$D(\omega) = \begin{cases} 1 & 0 \leq \omega \leq \omega_p \\ 0 & \omega_s \leq \omega \leq \pi. \end{cases} \tag{18}$$

The $\mathcal{L}_\infty$-norm is necessary because it ensures that the maximum error within the entire stop band region is minimized. In other words, it puts heavy emphasis on the undesirable spur from baseline design. Notice, however, the optimization setup is highly nonlinear and involved a $M$-th order polynomial in the optimization variable $\mathbf{d}$.

Although such problem formulation cannot be solved using any standard convex optimization solver, we can reach a reasonable optimal through gradient descent approaches given an ideal starting point [27]. Notice that $\gamma = 1$ converts the formulation back into the original signal process allpass filter bank setup. The effect of $\gamma$ can therefore be viewed as a perturbation on the optimal solution obtained from the DSP approach, and the coefficients from the original design

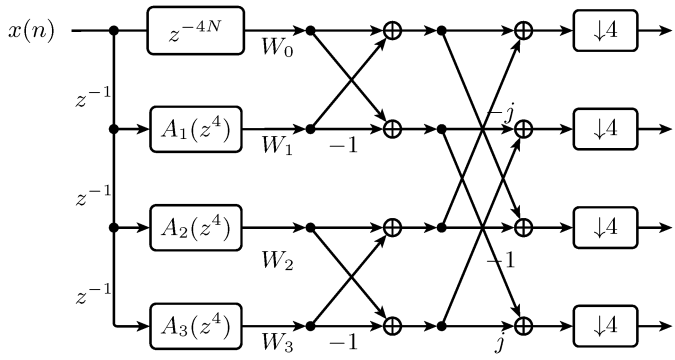


Fig. 9. Example signal flow for a four-channel allpass based photonic filter.

can be used as a starting point to the iterative algorithm. The overall design algorithm is presented in Algorithm 1.

An example signal flow diagram of a 4-channel DFT allpass filter bank is shown in Fig. 9. The implementation of Fig. 9 as an optical integrated circuit is straight forward from the diagram. The delays $z^{-1}$'s are simple specific-length sections of waveguides. The allpass sections are fourth-order ring-resonator lattices, as diagrammed in Fig. 1. The splitters and combiners can be implemented as y-junctions, which have an intrinsic attenuation of 3 dB per junction plus an excess loss of 0.2 $\sim$ 2 dB [28]. The crossings in the diagram, while not usually taken literally in a signal flow diagram, are implemented as actual waveguide crossings, which have been shown to exhibit an insertion loss as low as 0.02 dB [29]. Note that any additional loss incurred on the signal by the structure can be considered as a congregated loss term on the branch weights. Further notice that the partial signal from each allpass filter traverses through the same number of y-junctions, splitters, and crossings at any given output port. The implementation losses therefore simply result in an attenuation in the overall response, and do not affect the fidelity of the filters. In addition, any degree of randomness to the losses in the structure can be treated through error analysis.

## Algorithm 1: Photonic Allpass Filter Bank

**Given**: filter order $N$, number of channels $M$, waveguide power loss $\gamma$, passband and stopband frequencies $\omega_p$, $\omega_s$.
compute initial allpass filter coefficients based on [26] and initial weights according to (12).
use computed results as an initial guess for a gradient descent algorithm on (17).

## 5. Example Results

To demonstrate the performance of the proposed algorithm, we first compare our results to that of the classic allpass filter bank design. Fig. 10 shows the comparison results for the magnitude response of the baseband analysis filter $H_0(z)$ for a 4-channel filter bank. In this example, $N = 2$, $\omega_p = 0.2\pi$, and $\gamma = 0.97$, which corresponds to $-0.11$ dB per 90 degree turn in a ring resonator based setup. The poles and zeros of the proposed and traditional designs are shown in Fig. 11. Notice that proposed algorithm is able to place the roots close to the unit circle despite the effect of loss, thus providing improved attenuation and sharper transition band. The proposed design algorithm is able to decrease the spur level by $>$ 10 dB while maintaining the specifications, enabling the allpass based filter bank structure for photonic implementation. The allpass based structure is also able to provide linear phase, which is crucial in higher order modulation schemes such as MPSK and QAM.

Fig. 12 shows an example 8-channel design and the effect of randomness in loss from the arithmetic elements. In this example, $N = 6$, $\omega_p = 0.115\pi$, and $\gamma = 0.97$. The effect of loss is

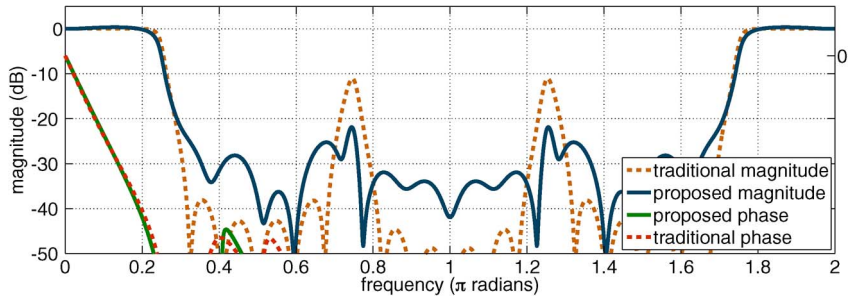


Fig. 10. Magnitude response of $H_0(z)$ in a 4-channel DFT allpass filter bank when implemented using photonic elements with a loss of $\gamma = 0.97$ using the proposed algorithm.

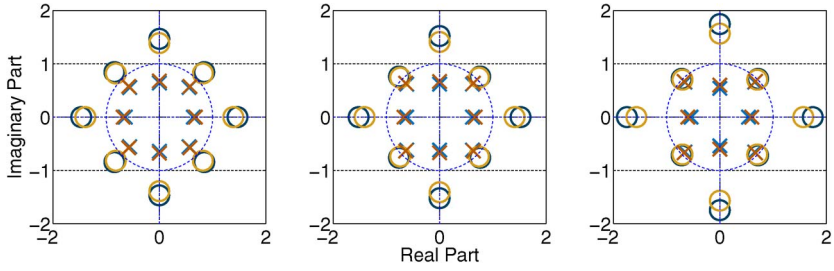


Fig. 11. Poles and zeros of the allpass filters $A_k(z^4)$ in a 4-channel filter bank from the proposed (gold) and the traditional (blue) designs after incorporating $\gamma$.

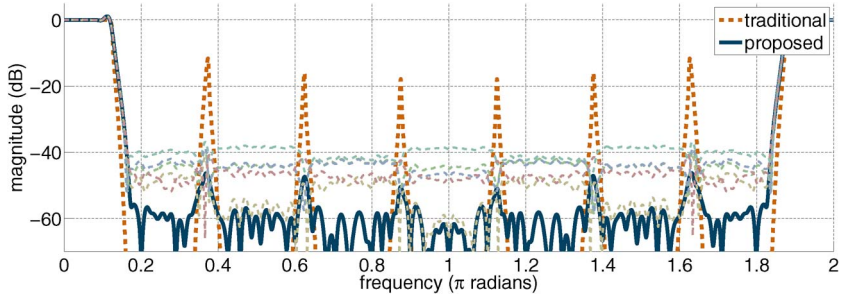


Fig. 12. Magnitude response of $H_0(z)$ in a 8-channel DFT allpass filter bank when additional losses from the arithmetic elements are considered. Note that the filter bank shows $-50$ dB of stopband attenuation when the losses from the elements are uniform and $\sim -40$ dB, even when each branch contains up to $\sim$0.05 dB of random additional loss.

simulated as a random attenuation on the branch weights drawn from Gaussian distribution with 0.05 dB standard deviation. The average of the losses is ignored since it would simply cause the plot to exhibit a downward shift in the vertical direction, which can be subsequently normalized. Through this simple error analysis, it can be seen that the structure is able to tolerate non-uniformity as well as nominal losses from the y-junctions, splitters, and crossings.

In WDM applications, it is often necessary to have a large number of channels in the filter bank setup for high density packing. Figs. 13 and 14 show the example baseband response for a 24 channel allpass filter bank and its corresponding spectra for all channels for a waveguide loss of $\gamma = 0.95$ and $N = 2$. As shown by the figures, the proposed design algorithm is able to remove the spurs with no additional follow-up filtering. The results suggest that an attenuation of more than 30 dB can be achieved using only two rings for each allpass filter. Also notice that unlike a sequential filtering approach, all 24 channels have identical responses due to the enforced constraint from the structural setup.

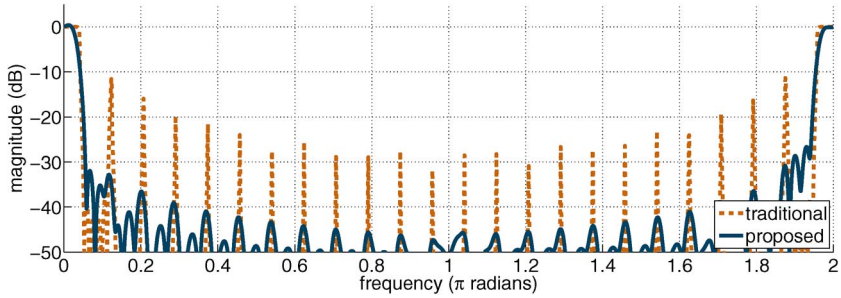


Fig. 13. Magnitude response of $H_0(z)$ in a 24-channel DFT allpass filter bank with $\gamma = 0.95$.

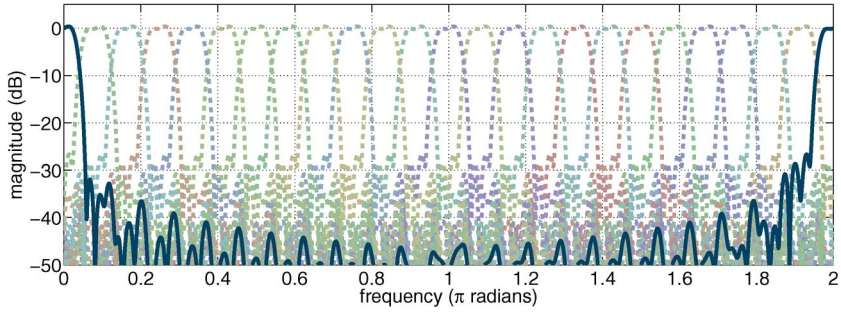


Fig. 14. Spectra for all analysis filters in a 24-channel filter bank.

While the proposed algorithm can be applied to systems with any amount of loss in theory, the performance improvement is most prominent for $\gamma \geq 0.9$, which are observed in realistic ring based architectures [20]. Since the optimization setup considers the design of a *M*-channel filter bank as a whole, the waveguide loss is effectively decoupled from other design parameters. As with all filter design algorithms, increasing filter order *N* and increasing the transition bandwidth result in better performance by providing the algorithm with more degrees of freedom.

## 6. Conclusion

This paper presents the structure and design of a filter bank setup specifically for photonic implementation. The proposed structure is completely based on allpass elements, which are naturally observed in a variety of nanoscale photonic dielectric components. The system is also optimized such that it can be readily combined with techniques such as time-stretching to reduce the implementation complexity and improve the filtering performance. While similar design exists in the digital signal processing domain, the structure requires further filtering due to the presence of undesirable spurs. We present a novel design technique that optimally utilizes the waveguide loss to mitigate the inherent challenges of the structure. The proposed algorithm based on both convex and nonlinear optimization techniques shows that the resulting allpass based filter bank can be derived without any additional hardware. The presented structure is ideal for higher order modulation schemes and high-speed time stretch ADCs that require superior filtering needs with large number of channels and constant group delay.

## References

[1] C. K. Madsen, "General IIR optical filter design for WDM applications using all-pass filters," *J. Lightw. Technol.*, vol. 18, no. 6, pp. 860–868, Jun. 2000.

[2] F. Horst *et al.*, "Cascaded Mach–Zehnder wavelength filters in silicon photonics for low loss and flat pass-band WDM (de-)multiplexing," *Opt. Exp.*, vol. 21, no. 10, pp. 11 652–11 658, May 2013.

[3] R. Aguinaldo *et al.*, "Wideband silicon-photonic thermo-optic switch in a wavelength-division multiplexed ring network," *Opt. Exp.*, vol. 22, no. 7, pp. 8205–8218, Apr. 2014.
[4] Y. Han and B. Jalali, "Photonic time-stretched analog-to-digital converter: Fundamental concepts and practical considerations," *J. Lightw. Technol.*, vol. 21, no. 12, pp. 3085–3103, Dec. 2003.
[5] B. H. Verbeek *et al.*, "Integrated four-channel Mach–Zehnder multi/demultiplexer fabricated with phosphorous doped $SiO_2$ waveguides on si," *J. Lightw. Technol.*, vol. 6, no. 6, pp. 1011–1015, Jun. 1988.
[6] Y. A. Vlasov and S. J. McNab, "Losses in single-mode silicon-on-insulator strip waveguides and bends," *Opt. Exp.*, vol. 12, no. 8, pp. 1622–1631, Apr. 2004.
[7] Y. Wang, A. Grieco, and T. Nguyen, "Allpass filter design with waveguide loss compensation," *Opt. Exp.*, vol. 21, no. 26, pp. 32 040–32 052, Dec. 2013.
[8] Y. Wang, R. Aguinaldo, and T. Nguyen, "Realistic photonic filter design based on allpass substructures with waveguide loss compensation," *J. Lightw. Technol.*, vol. 32, no. 5, pp. 1024–1031, Mar. 2014.
[9] A. Rigny, A. Bruno, and H. Sik, "Multigrating method for flattened spectral response wavelength multi/demultiplexer," *Electron. Lett.*, vol. 33, no. 20, pp. 1701–1702, Sep. 1997.
[10] Z. Shi, J.-J. He, and S. He, "An analytic method for designing passband flattened DWDM demultiplexers using spatial phase modulation," *J. Lightw. Technol.*, vol. 21, no. 10, pp. 2314–2321, Oct. 2003.
[11] S.-W. Park, Y. Park, Y. Yi, and H. Kim, "Iterative method for optimal design of flat-spectral-response arrayed waveguide gratings," *Appl. Opt.*, vol. 52, no. 30, pp. 7295–7301, Oct. 2013.
[12] P. P. Vaidyanathan, *Multirate Systems and Filter Banks*. Karnataka, India: Pearson Education India, 1993.
[13] J. Bae and J. Chun, "Design of fiber bragg gratings using the simulated annealing technique for an ideal WDM filter bank," in *Proc. 21st IEEE MILCOM*, 2000, vol. 2, pp. 892–896.
[14] G. Cincotti, "Full optical encoders/decoders for photonic IP routers," *J. Lightw. Technol.*, vol. 22, no. 2, pp. 337–342, Feb. 2004.
[15] G. Cincotti and A. Neri, "Logarithmic wavelength demultiplexers," *J. Lightw. Technol.*, vol. 21, no. 6, pp. 1576–1583, Jun. 2003.
[16] T. E. Tuncer and T. Q. Nguyen, "Interpolated LIR Mth-band filter design with allpass subfilters," *IEEE Trans. Signal Process.*, vol. 43, no. 8, pp. 1986–1990, Aug. 1995.
[17] A. Canciamilla *et al.*, "Silicon coupled-ring resonator structures for slow light applications: Potential, impairments and ultimate limits," *J. Opt.*, vol. 12, no. 10, pp. 104008-1–104008-7, Oct. 2010.
[18] H. C. Kim, K. Ikeda, and Y. Fainman, "Resonant waveguide device with vertical gratings," *Opt. Lett.*, vol. 32, no. 5, pp. 539–541, Mar. 2007.
[19] F. Harris, E. Venosa, X. Chen, P. Kumar, and C. Dick, "Comparison of standard low pass filter types in two-path half-band IIR filter structures," in *Proc. ISSCS*, 2013, pp. 1–4.
[20] R. Aguinaldo, Y. Shen, and S. Mookherjea, "Large dispersion of silicon directional couplers obtained via wideband microring parametric characterization," *IEEE Photon. Technol. Lett.*, vol. 24, no. 14, pp. 1242–1244, Jul. 2012.
[21] F. P. Payne and J. P. R. Lacey, "A theoretical analysis of scattering loss from planar optical waveguides," *Opt. Quantum Electron.*, vol. 26, no. 10, pp. 977–986, Oct. 1994.
[22] R. Soref and B. Bennett, "Electrooptical effects in silicon," *IEEE J. Quantum Electron.*, vol. 23, no. 1, pp. 123–129, Jan. 1987.
[23] J. Azana and L. R. Chen, "Multiwavelength optical signal processing using multistage ring resonators," *IEEE Photon. Technol. Lett.*, vol. 14, no. 5, pp. 654–656, May 2002.
[24] C. K. Madsen and J. H. Zhao, *Optical Filter Design and Analysis*. Hoboken, NJ, USA: Wiley-Interscience, 1999.
[25] A. M. Prabhu and V. Van, "Predistortion techniques for synthesizing coupled microring filters with loss," *Opt. Commun.*, vol. 281, no. 10, pp. 2760–2767, May 2008.
[26] T. Q. Nguyen, T. I. Laakso, and R. D. Koilpillai, "Eigenfilter approach for the design of allpass filters approximating a given phase response," *IEEE Trans. Signal Process.*, vol. 42, no. 9, pp. 2257–2263, Sep. 1994.
[27] A. Antoniou, *Digital Filters*. New York, NY, USA: McGraw-Hill, 1993.
[28] Y. Zhang *et al.*, "A compact and low loss Y-junction for submicron silicon waveguide," *Opt. Exp.*, vol. 21, no. 1, pp. 1310–1316, Jan. 2013.
[29] Y. Zhang, A. Hosseini, X. Xu,D. Kwong, and R. T. Chen, "Ultralow-loss silicon waveguide crossing using Bloch modes in index-engineered cascaded multimode-interference couplers," *Opt. Lett.*, vol. 38, no. 18, pp. 3608–3611, Sep. 2013.